

# **In-situ optical measurement of charge transport dynamics in organic photovoltaics**

Philip C.Y. Chow, Sam L. Bayliss, Girish Lakhwani <sup>§</sup>, Neil C. Greenham, Richard H. Friend\*

Cavendish Laboratory, University of Cambridge, J J Thomson Avenue, Cambridge, United Kingdom

§ Present address: School of Chemistry, University of Sydney, NSW, Australia

## **Abstract**

We present a novel experimental approach which allows extraction of both spatial and temporal information of charge dynamics in organic solar cells. Using the wavelength dependence of the photonic structure in these devices, we monitor the change in spatial overlap between the photogenerated hole distribution and the optical probe profile as a function of time. In a model system we find evidence for a build-up of the photogenerated hole population close to the hole-extracting electrode on a nanosecond timescale, and show that this can limit charge transport through space-charge effects under operating conditions.

**Keywords:** photovoltaics, solar cells, organic, charge transport, optical spectroscopy, transient absorption

## Main text

Bulk heterojunction organic photovoltaics (OPVs) are promising candidates for next-generation solar cell technology due to their simple and low-cost fabrication methods, and power conversion efficiencies above 10% have now been achieved [1]. Understanding the dynamics of photogenerated charges has long been an important question from both a scientific and a technological point of view, and a particularly useful experimental technique for this purpose is transient absorption (TA) spectroscopy. These measurements, which are typically performed with thin-film samples of donor-acceptor blends, enable the population of photoexcited states such as charges to be studied as a function of time [2-6]. While this technique has been instrumental to our current understanding of charge dynamics in OPVs, it has been, however, limited by: 1) the lack of spatial information of the population distribution, 2) the absence of net electric field across the system (analogous to the flat-band condition), and 3) the inability to account for any interfacial effects induced by contact electrodes which can be important in operational devices [7-9]. Here we present a novel experimental approach which tackles these limitations, and use it to provide evidence for a build-up of hole population close to the hole-extracting electrode for a model OPV system.

A schematic of the experimental technique is shown in Figure 1. The two optical beams, depicted as ‘pump’ and ‘probe’, are directed through the semi-transparent layers of a fully encapsulated OPV device, and reflected off the aluminium back electrode. For the device architecture used for this study (see Methods), the active layer thickness ( $d = 100$  nm) is less than the illuminating wavelengths and the optical field must vanish at the metallic back electrode. This creates a significant spatial variation of the optical generation profile across the device, and therefore a non-uniform charge distribution. We simulated the optical profiles of both pump and probe beams created inside the active layer using a transfer matrix formalism based on optical constants measured using spectroscopic ellipsometry [10]. At 532 nm we find that the pump beam predominantly generates photoexcitations near the centre of the active layer, while the probe, with a

wavelength of 1000 nm selected to detect the absorption associated with hole polarons, preferentially probes photoexcitations near the hole-extracting electrode, which comprises a thin layer of poly(3,4-ethylenedioxythiophene):poly(styrenesulfonic acid) (PEDOT:PSS) deposited on an indium tin oxide (ITO) substrate. The transient absorption response of the reflected probe beam ( $\Delta T/T$ ) due to photoexcitations created by the pump is determined by the overlap of the probe optical profile with the photoexcitation profile: [Equation 1]

$$\Delta T/T(t) \propto \int_0^d N(x,t) P(x) dx$$

where  $x$  denotes the direction perpendicular to the plane of the device,  $N(x,t)$  is the spatial distribution of the photoexcitations generated by the pump beam as a function of time and  $P(x)$  is the (non-uniform) optical profile of the probe beam. Since the overlap of the photoexcitation density and the probe depends on the spatial distribution of  $N(x,t)$ , this makes our measurement sensitive not only to the temporal dynamics of photoexcitations, but also to their spatial evolution. Although TA measurements under reflection mode in OPV systems have been previously reported [11,12], the non-uniform optical profile and its effect on the signal response, which we show below to be of critical importance, have not yet been explored (except in a recent study by MacKenzie et al. to explain transient electroabsorption measurements [13]).

The active layer of the system studied here comprises a blend of poly[2,6-(4,4-bis-(2-ethylhexyl)-4H-cyclopenta-[2,1-b;3,4-b']-dithiophene)-alt-4,7-(2,1,3-benzothiadiazole)] (PCPDTBT [14]), which acts as the donor polymer, and phenyl-C<sub>71</sub>-butyric acid methyl ester (PC<sub>70</sub>BM [15]), which acts as the fullerene acceptor. The blend morphology (and therefore the PV performance) is empirically optimised through the use of the solvent additive 1,8-octanedithiol (ODT) [16]. The photophysics of this materials combination has been well studied [4,5], and it therefore acts as an ideal model system for this work.

Figure 2a shows the time dependence of the optical response at 1000 nm for a range of bias voltages, all at a low excitation fluence of 1  $\mu\text{J}/\text{cm}^2$ . Since the

absorption cross-section of the electron polaron on the fullerene acceptor is much smaller than that of the hole polaron on the polymer [17], the optical response is primarily due to absorption of holes on the donor (with a contribution also from spin-triplet excitons formed by bimolecular recombination [4]). The fall-off of the response beyond 100 ns is due both to recombination and, at increasing negative bias, to charge extraction. We observe a significant rise in the polaron response at negative bias voltages, with an increase in response of about 25% at 100 ns at -1.5 V bias. It is this rising response that provides the critical observation for this paper, and we demonstrate below that this is due to build-up of holes close to the PEDOT:PSS electrode as they drift from their point of photogeneration near the centre of the device to this electrode at which the probe response is larger. This growth in response is only seen when the excitation fluence is low, as shown in Figure 2b.

We concentrate our examination of this increased hole absorption response on the low-fluence case ( $1 \mu\text{J}/\text{cm}^2$ ) at -1.5 V bias. Under these conditions, the quantum yield for charge collection is high (above 75% [18]) because electrons and holes drift rapidly away from one another, limiting the effect of bimolecular recombination (which would be evident as the growth of a triplet exciton population [4]). Therefore, under these conditions most holes are eventually extracted, and the transient rise in their optical response is due (as we model below) to hole accumulation at the PEDOT:PSS electrode. At lower reverse bias voltages or under forward bias, where the electric field across the bulk of the device is reduced and charge carrier diffusion becomes increasingly important over drift, this new response disappears. We consider that this is due to faster recombination induced by the increased spatial overlap between electrons and holes. This is also reflected in the drop in quantum yield from above 75% at -1.5V bias to 65% at short-circuit [4, 18]. We therefore consider it likely that holes also accumulate at the electrode at device operating voltages despite the fact that an overall rising signal was not observed under these bias conditions. Similarly, the response is quickly quenched at higher excitation fluences due to an increased rate of bimolecular recombination as reflected in the rapid drop in quantum yield (See Supporting Information). We note that we find similar evidence for hole accumulation under reverse bias conditions for systems with other donor polymers, including PTB7, P3HT and PCDTBT (see Supporting Information), indicating this as a general behaviour in model high-efficiency OPV devices.

We model the observed hole absorption response using a numerical drift-diffusion model, as described in detail in Ref. [19]. To model hole accumulation, we introduce a trap population adjacent to the PEDOT:PSS electrode, and the drift-diffusion equations are solved by dividing the total hole density  $p$  into ‘free’  $p_f$  and ‘trapped’  $p_t$  hole densities. The change in free hole density as a function of time is given by: [Equation 2]

$$\frac{\partial p_f}{\partial t} = \frac{1}{q} \frac{\partial}{\partial x} \left[ p_f \mu q E - \mu k_B T \frac{\partial p_f}{\partial x} \right] - \frac{\partial p_t}{\partial t}$$

with average hole mobility  $\mu$ , electric charge  $q$ , electric field  $E$ , and thermal energy  $k_B T$ . The dynamics of the trapped holes are governed by the trapping and de-trapping of free holes into and from the total density of trapping sites,  $P_t$ , with a trapping rate constant,  $C_t$ , and de-trapping rate constant,  $C_{dt}$ : [Equation 3]

$$\frac{\partial p_t}{\partial t} = C_t (P_t - p_t) p_f - C_{dt} p_t$$

These trapping sites, with a single trapping energy level, are fixed adjacent to the PEDOT:PSS electrode such that all holes must go through them in order to be extracted. We emphasise that these interfacial traps are introduced as a computational tool to influence the extraction rate of the holes, and do not necessarily correspond to physical trap populations. We consider that electron extraction is not delayed since similar PV performance is observed with Ca/Al and Al electron-extracting electrodes [7]. For simplicity we neglect the nanoscale blend morphology and take the initial charge profile as that of the pump beam shown in Figure 1b. Furthermore we neglect recombination, which is expected to be small as is evident from the high quantum yield for charge collection of above 75% at -1.5 V bias [18].

Using an average hole mobility of  $\mu = 5 \times 10^{-8} \text{ m}^2/\text{Vs}$ , which is in good agreement with that reported previously by Lenes et al. [20], a total trap site density of  $P_t = 10^{25} \text{ m}^{-3}$ , and trapping and de-trapping rate constants of  $C_t = 2 \times 10^{-15} \text{ m}^3 \text{ s}^{-1}$  and  $C_{dt} = 5 \times 10^8 \text{ s}^{-1}$  (giving a ratio  $P_t C_t / C_{dt}$ , of 40), the model qualitatively reproduces

the response observed in the experimental data (blue solid line in Figure 3). The dashed line shows the modelled response assuming a uniform probe optical field within the device. This represents the normalised response of the total hole population ( $p$ ) in the device, which remains nearly constant before extraction occurs on a timescale of about 100 ns (with recombination suppressed at reverse bias). Since the hole mobility determines the timescale on which holes reach the PEDOT:PSS electrode, this determines the rise time of the optical response. We note that the numerical values of  $P_t$ ,  $C_t$  and  $C_{dt}$  used above are coupled, since the overall kinetics depends on the ratio  $P_t C_t / C_{dt}$ , and merely act to tune the extraction rate (see Supporting Information). In this case the ratio is 40, which indicates that it is highly likely for holes to be trapped at least once before leaving the device, and therefore accumulate close to the PEDOT:PSS electrode prior to extraction. This is consistent with previous studies showing that PEDOT:PSS presents a blocking electrode unless treated with polar non-solvents such as methanol [7-9]. We note that for devices which are not extraction limited, it is expected that the rise in response would be less significant than that observed for the model system studied herein.

We now discuss the effect of such hole accumulation on the charge extraction efficiency of the device. As shown in Figure 2b, the rising hole absorption response is only observed at low fluence ( $1 \mu\text{J}/\text{cm}^2$  per pulse at 532 nm). At such a fluence the instantaneous excitation density created within the system is about  $10^{17} \text{ cm}^{-3}$ , which is comparable to the charge density typically found in operating devices under solar illumination (at open-circuit conditions the excess photocarrier density is typically between  $10^{16} - 10^{17} \text{ cm}^{-3}$  [21]). At higher fluences the rising response is destroyed by faster recombination processes due to the increased charge densities, in accord with the fact that the device quantum efficiency drops rapidly as the fluence exceeds solar conditions [11] (See Supporting Information). We consider that recombination processes are enhanced by space-charge effects due to the accumulation of holes at the PEDOT:PSS electrode. We note that space-charge effects have previously been posited as an explanation for why it is difficult to make optically thick OPV devices and why it is important to raise the bulk mobility of the active layer above a threshold value [22]. Using the fitting parameters above, we attempt to quantify the space-charge effects by modelling the drop in electric potential across the bulk of the device (excluding the narrow region next to the PEDOT:PSS where the traps are located)

calculated under short-circuit and steady-state conditions as a function of charge density (See Supporting Information). We find that at low charge densities ( $< 10^{15} \text{ cm}^{-3}$ ), the space-charge effects are weak and the electric potential across the bulk is close to the built-in voltage of 0.6 V. However, at charge densities typically found in OPV devices under solar illumination, the space-charge effects become significant and the electric potential across the bulk can drop to below half of the built-in voltage. This electric field screening can limit charge transport and thus increase recombination, therefore limiting device performance [22].

By utilising the non-uniform optical profiles of the pump and probe pulses generated across the active layer, we have presented a novel experimental approach which allows extraction of both spatial and temporal information of charge transport dynamics in fully encapsulated, operating OPV devices. We have applied this technique to provide evidence for hole accumulation close to the PEDOT:PSS electrode prior to extraction in PCPDTBT:PC<sub>70</sub>BM devices, which is consistent with experiments showing that PEDOT:PSS can act as a blocking electrode [7-9]. We have shown that such build-up of hole population can limit charge transport and increase recombination rates through space-charge effects at charge densities typically found in operating devices. Minimising such hole accumulation is thus necessary to further improve the device efficiency of OPVs. Finally, we consider that the spatial and temporal information afforded by the experimental technique introduced here can be useful for understanding the transport dynamics of photoexcited states in a wide range of photovoltaic systems, including charges in perovskite-based solar cells [23] and triplet excitons/charges in singlet-fission sensitised solar cells [24].

## **Methods**

*Device fabrication:* PEDOT:PSS solution (acquired from Heraeus (Clevios PH1000)) was spin-coated onto pre-cleaned indium tin oxide (ITO) glass, followed by post-deposition thermal annealing at 150 °C for 30 min under nitrogen flow. The PCPDTBT:PC<sub>70</sub>BM active layer was then deposited by spin-coating from a 30 mg/ml solution dissolved in chlorobenzene at 1:2 weight ratio with ODT (2.4% volume ratio) onto the PEDOT:PSS/ITO substrate inside a nitrogen glovebox. On the other end of

the device, a 100 nm-thick aluminium layer was thermally evaporated onto the active layer. To ensure a smooth contact, the aluminium was deposited at a rate of 0.1 nm/s. The devices were then encapsulated in epoxy resin to avoid exposure to air.

*Transient absorption spectroscopy:* The pump pulses (at 532 nm) were generated using the second harmonic output of a Q-switched Nd:YVO<sub>4</sub> laser (ACE; Advanced Optical Technologies Ltd.). The probe pulses (at 1000 nm) were generated using home-built non-collinear optical parametric amplifiers (NOPA) seeded with a portion of the output of a Ti:sapphire amplifier system (Spectra-Physics Solstice) operating at 1 kHz. The pump and probe beams are focused and overlapped on a device pixel, and reflected off the aluminium back electrode. Laser fluctuations were normalized by splitting a portion of the probe beam into a reference beam, which is also focused onto the device pixel in a region not affected by the pump. The reflected probe and reference beams were dispersed in a spectrometer (Andor, Shamrock SR- 303i) and detected using a pair of 16-bit, 512-pixel linear image sensors (Hamamatsu). A custom-built board enabled data acquisition at 1 kHz, and the differential transmission signal ( $\Delta T/T$ ) was calculated after accumulating and averaging 1000 pump-on and pump-off shots for each data point.

*Drift-diffusion simulation:* Hole polaron density was calculated as a function of time, using equations as described in detail in Ref. [19]. We solved the drift-diffusion continuity equations for both electrons and holes by dividing the 100 nm-thick light-absorbing layer into 101 points on a spatial grid, and integrating forward in time. For simplicity, we ignored the nanoscale blend morphology and take the initial charge profile as that of the pump beam. We also neglected recombination, which is weak under reverse bias voltages. The Scott-Malliaras injection model [25] was used to simulate the injection and extraction of charges.

## **Supporting Information**

Supporting Information Available: 1) Transient absorption (TA) measurements of devices with donor polymer P3HT, PTB7 and PCDTBT blended with PCBM. 2) Influence of de-trapping rate constant on simulated TA kinetics. 3) Fluence dependence of device photocurrent. 4) Device characterisation. 5) Change in electric potential across the bulk of device due to space-charge effect as a function of charge density. This material is available free of charge via the Internet at <http://pubs.acs.org>.

## **Author Information**

Corresponding Author

\*Email: [rhf10@cam.ac.uk](mailto:rhf10@cam.ac.uk)

Notes

The authors declare no competing financial interest.

## **Acknowledgements**

This work was supported by the EPSRC [Grant number EP/G060738/1].

## References

- (1) Scharber, M. C.; Sariciftci, N. S. *Progress in Polymer Science* **2013**, *38*, 1929–1940.
- (2) Kaake, L. G.; Sun, Y.; Bazan, G. C.; Heeger, A. J. *Appl. Phys. Lett.* **2013**, *102*, 133302.
- (3) Rao, A.; Chow, P. C. Y.; Gélinas, S.; Schlenker, C. W.; Li, C.-Z.; Yip, H.-L.; Jen, A. K.-Y.; Ginger, D. S.; Friend, R. H. *Nature* **2013**, *500*, 435–439.
- (4) Chow, P. C. Y.; Gélinas, S.; Rao, A.; Friend, R. H. *J. Am. Chem. Soc.* **2014**, *136*, 3424–3429.
- (5) Etzold, F.; Howard, I. A.; Forler, N.; Cho, D. M.; Meister, M.; Mangold, H.; Shu, J.; Hansen, M. R.; Müllen, K.; Laquai, F. *J. Am. Chem. Soc.* **2012**, *134*, 10569–10583.
- (6) Shivanna, R.; Shoaee, S.; Dimitrov, S.; Kandappa, S. K.; Rajaram, S.; Durrant, J. R.; Narayan, K. S. *Energy Environ. Sci.* **2014**, *7*, 435–441.
- (7) Kumar, A.; Lakhwani, G.; Elmalem, E.; Huck, W. T. S.; Rao, A.; Greenham, N. C.; Friend, R. H. *Energy Environ. Sci.* **2014**, *7*, 2227.
- (8) Zhou, H.; Zhang, Y.; Seifert, J.; Collins, S. D.; Luo, C.; Bazan, G. C.; Nguyen, T.-Q.; Heeger, A. J. *Adv. Mater.* **2013**, *25*, 1646–1652.
- (9) Tan, Z.-K.; Vaynzof, Y.; Credgington, D.; Li, C.; Casford, M. T. L.; Sepe, A.; Huettner, S.; Nikolka, M.; Paulus, F.; Yang, L.; Siringhaus, H.; Greenham, N. C.; Friend, R. H. *Adv. Funct. Mater.* **2014**, *24*, 3051–3058.
- (10) Burkhard, G. F.; Hoke, E. T.; McGehee, M. D. *Adv. Mater.* **2010**, *22*, 3293–3297.
- (11) Marsh, R. A.; Hodgkiss, J. M.; Friend, R. H. *Adv. Mater.* **2010**, *22*, 3672–3676.
- (12) Jamieson, F. C.; Agostinelli, T.; Azimi, H.; Nelson, J.; Durrant, J. R. *J. Phys. Chem. Lett.* **2010**, *1*, 3306–3310.
- (13) MacKenzie, R. C. I.; Göritz, A.; Greedy, S.; Hauff, von, E.; Nelson, J. *Phys. Rev. B* **2014**, *89*, 195307.
- (14) Mühlbacher, D.; Scharber, M.; Morana, M.; Zhu, Z.; Waller, D.; Gaudiana, R.; Brabec, C. *Adv. Mater.* **2006**, *18*, 2884–2889.
- (15) Sariciftci, N. S.; Smilowitz, L.; Heeger, A. J.; Wudl, F. *Science* **1992**, *258*, 1474–1476.
- (16) Peet, J.; Kim, J. Y.; Coates, N. E.; Ma, W. L.; Moses, D.; Heeger, A. J.; Bazan, G. C. *Nature Materials* **2007**, *6*, 497–500.
- (17) Chow, P. C. Y.; Albert-Seifried, S.; Gélinas, S.; Friend, R. H. *Adv. Mater. Weinheim* **2014**, *26*, 4851–4854.
- (18) Albrecht, S.; Schäfer, S.; Lange, I.; Yilmaz, S.; Dumsch, I.; Allard, S.; Scherf, U.; Hertwig, A.; Neher, D. *Organic Electronics* **2012**, *13*, 615–622.
- (19) Hwang, I.; McNeill, C. R.; Greenham, N. C. *Journal of Applied Physics* **2009**, *106*, 094506.
- (20) Lenes, M.; Morana, M.; Brabec, C. J.; Blom, P. W. M. *Adv. Funct. Mater.* **2009**, *19*, 1106–1111.
- (21) Credgington, D.; Hamilton, R.; Atienzar, P.; Nelson, J.; Durrant, J. R. *Adv. Funct. Mater.* **2011**, *21*, 2744–2753.
- (22) Lakhwani, G.; Rao, A.; Friend, R. H. *Annu. Rev. Phys. Chem.* **2014**, *65*, 557–581.
- (23) Kazim, S.; Nazeeruddin, M. K.; Grätzel, M.; Ahmad, S. *Angew. Chem. Int. Ed. Engl.* **2014**, *53*, 2812–2824.

- (24) Tabachnyk, M.; Ehrler, B.; Bayliss, S.; Friend, R. H.; Greenham, N. C. *Appl. Phys. Lett.* **2013**, *103*, 153302.
- (25) Scott, J. C.; Malliaras, G. G. *Chemical Physics Letters* **1999**, *299*, 115-119.

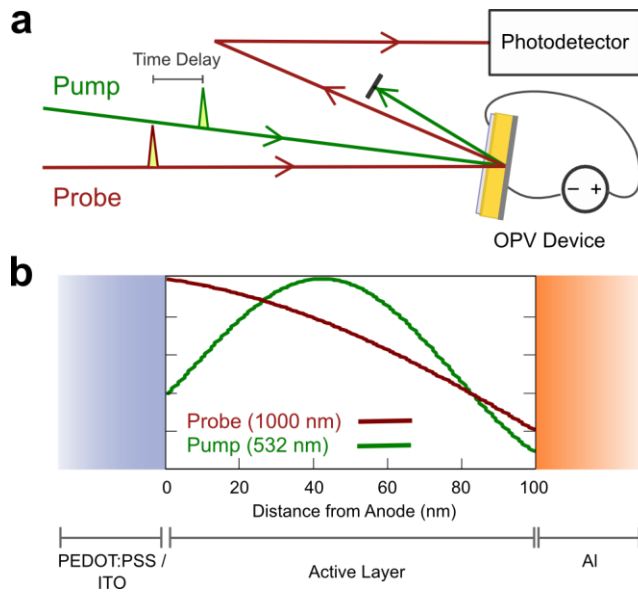


**Figure 1.** (a) Schematic of transient absorption measurement on encapsulated OPV device under an applied bias. The pump and probe beams are focussed onto the same spot on the device pixel, and reflected off the aluminium back electrode. The reflected probe beam is subsequently directed to the photodetector. The time delay between the pump (with 1 ns pulse width) and the probe pulse (with <1 ps pulse width) is achieved electronically. (b) Optical profiles of the pump and probe beams created inside the light-absorbing layer, calculated using a transfer matrix formalism based on optical constants obtained by spectroscopic ellipsometry. At their respective wavelengths, the pump generates excitations near the centre of the device, which evolve in time, while the probe preferentially monitors excitations near the PEDOT:PSS electrode. We obtain spatial and temporal information by monitoring the change in overlap between the photogenerated hole distribution and the optical probe profile as a function of time.

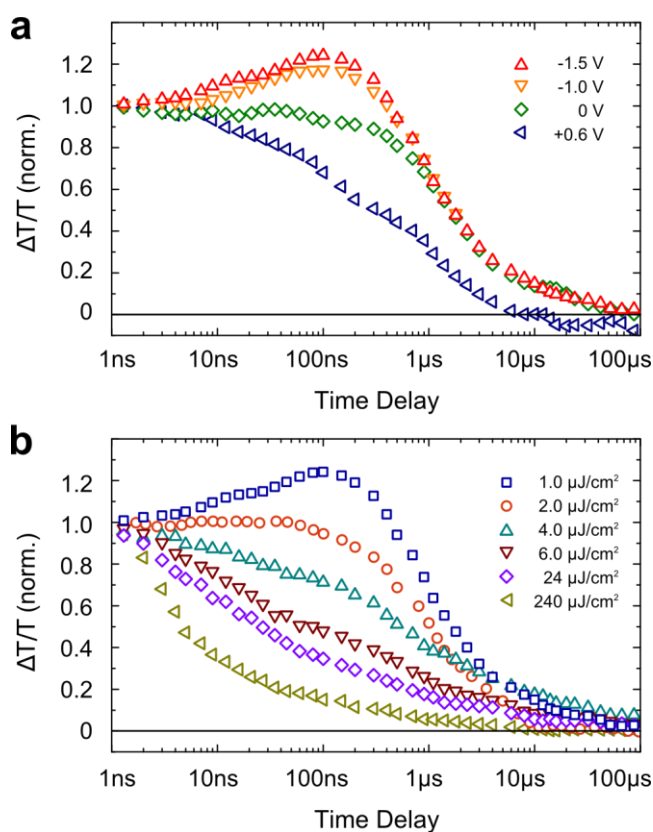


**Figure 2.** Transient absorption (TA) measurement of a PCPDTBT:PC<sub>70</sub>BM device, photoexcited at 532 nm and probed at 1000 nm, and normalised at 1 ns. The optical response corresponds to the photoinduced absorption of hole polarons on the donor polymer photoexcited by the pump. (a) Effect of applied voltage bias on the optical response as a function of time at a constant excitation fluence of  $1 \mu\text{J}/\text{cm}^2$  per pulse. The fall-off of the response beyond 100 ns is due to both recombination and, at increasing negative bias, to charge extraction. The rising response at negative bias voltages, as we discuss in the text, is due to build-up of the hole population close to the PEDOT:PSS electrode as holes drift from their point of photogeneration near the centre of the device to this electrode at which the probe response is larger. At lower reverse bias voltages or under forward bias, where the electric field across the bulk of the device is reduced and charge carrier diffusion becomes increasingly important over drift, this new response disappears due to faster recombination. (b) Effect of excitation fluence on the optical response as a function of time at constant negative bias of -1.5 V. The rising response is quickly destroyed at higher excitation fluences due to an increased rate of bimolecular recombination.

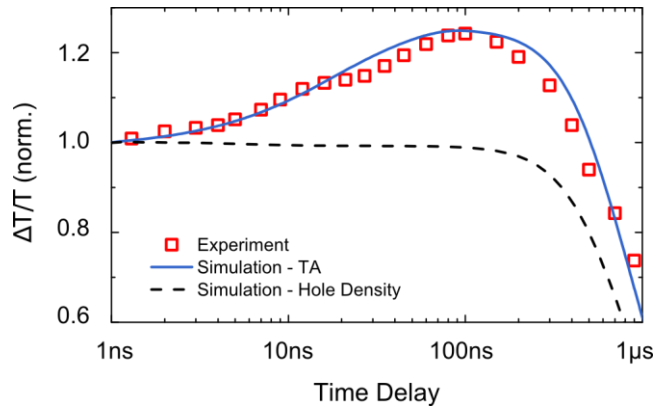


**Figure 3.** Modelling the optical response observed under low excitation fluence ( $1 \mu\text{J}/\text{cm}^2$ ) at negative bias ( $-1.5 \text{ V}$ ) using a numerical drift-diffusion transport model. By introducing a trapping layer adjacent to the PEDOT:PSS electrode, we find that the model (blue solid line) qualitatively simulates the observed response when a large population of holes are trapped before exiting the device. The rising response is thus due to holes drifting from their point of photogeneration near the centre of the device to the PEDOT:PSS electrode (at which the probe response is larger, as shown in Figure 1b), and then accumulate there until extraction occurs at 100 ns. Note that these interfacial traps are introduced as a computational tool to influence the extraction rate of the holes, and do not necessarily correspond to physical trap populations. The corresponding total hole population within the device is illustrated by the dashed line, which remains nearly constant (suppressed recombination) until extraction occurs.

# TOC figure

